Chapter 9

Radiative Impacts of Volcanic Aerosol in the Arctic

Cindy L. Young and Jennifer W. Telling

Additional information is available at the end of the chapter

http://dx.doi.org/10.5772/63421

Abstract

High latitude volcanic eruptions are high-frequency and intensity events capable of releasing large amounts of aerosols into the environment. Studies have shown that the Arctic is particularly sensitive to radiative perturbations due to aerosols, and a high sensitivity to volcanic aerosols would be expected. Despite the potential for volcanic aerosols to significantly perturb the Arctic radiation balance, the radiative impacts of volcanic aerosols in the Arctic are poorly understood and have received less attention than the effects of other aerosol types that are often present in the region, both natural and anthropogenic. A novel review of this topic is presented in detail in this chapter, focusing on the current state of the knowledge and the natural complexities involved with the problem, the important research tools, and the improvements that can be made over the status quo. The Arctic environment is both unique and complicated, and the perturbations caused by volcanic aerosol need to be examined in a regional context. An introduction to remote sensing and data collection in the Arctic is provided because there are often specific challenges, including high surface reflectivities, persistent meteorological clouds, the lack of winter daylight, and harsh conditions that hamper both in situ and remote data collection. Methods for tracking both aerosol and gas plumes in the Arctic that can help mitigate these issues are introduced. In addition to the physical constraints of data collection presented by the Arctic environment, volcanic aerosol is a complex mixture of varying aerosol compositions and sizes. Dealing with the nature of volcanic aerosol for optical calculations is further described, leading into a detailed discussion of the radiative impacts of volcanic plumes in the atmosphere. Radiative forcing comparisons of other aerosol types with comparable plume characteristics (e.g., thicknesses and optical depths) suggest that aerosol layers composed of significant proportions of volcanic ash can dominate the aerosol forcing in the region. Similar comparisons for ash deposits with other types of deposits that can be present in the region emphasize the ability of volcanic ash to produce large, and in some cases extreme, loadings that reduce albedo, which can have profound impacts on the Arctic radiation balance and hydrological cycle. The strengths and shortcomings of volcanic ash transport and dispersion models are reviewed and recommendations are made for future research that would strengthen the use of these models in Arctic environments. In particular, ash aggregation (or the sticking together of ash particles) is often not

considered fully in transport modeling, and the consequences of this are discussed. Finally, we present a review of secondary volcanic impacts to oceans and ecosystems that have not been constrained in an Arctic context but are potentially important to the Arctic environment and the global CO_2 cycle.

Keywords: Arctic, volcanic eruptions, ash, sulfate, remote sensing, transport modeling

1. Introduction

There is a strong need to understand the role natural aerosols play in modulating Arctic climate. The radiative impacts of smoke [1] and dust [2] have been considered. However, volcanic aerosols continue to be largely overlooked in the Arctic environment. The Arctic environment has a high sensitivity to radiative perturbations, as demonstrated by many previous studies of other types of aerosols (i.e., smoke, dust, and haze), and may be strongly sensitive to volcanic aerosols. This chapter defines the "Arctic region" to include the true Arctic (north of 66.5°N) and the sub-Arctic (50–66.5°N), because both areas are more sensitive to radiative perturbations than lower latitudes and aerosol can be easily transported between regions.

Volcanic eruptions are capable of producing a huge, sporadic aerosol signal, lasting from minutes to years [3], and high northern latitude eruptions can distribute aerosols over large areas, as evidenced by the 2010 eruption of Eyjafjallajökull in Iceland, which halted air transportation in much of Europe. The Alaska Volcano Observatory (AVO) reports that Alaskan volcanoes alone have had an average eruption frequency of two per year over the past 40 years. Depending on the time of year, volcanic aerosol may be present along with other aerosol types. Despite the high frequencies and intensities of volcanic eruptions, volcanic aerosols in the Arctic are relatively neglected in assessments of Arctic aerosol.

Volcanoes in the Arctic have been the source of many climatically important eruptions in the last several centuries. The June 1783 eruption of Laki, a volcanic fissure in Iceland, caused a drop in global temperatures [4], drought, and famine [5]. The June 1912 Novaerupta-Katmai eruption near Kodiak, Alaska, was the most powerful eruption of the 20th century, causing surface cooling in the Northern Hemisphere throughout the summers of 1912 and 1913 and a maximum surface cooling of −0.9°C for September 1912 [6]. Recent volcanic eruptions in the region include Redoubt (Alaska, USA) in March to April 2009, Sarychev (Russia) in June 2009, Shiveluch (Russia) in September 2009, Eyjafjallajökull (Iceland) in April to May 2010, and Plosky Tolbachik (Russia) in 2012 to 2013. Recent and ongoing eruptions in the Arctic have fortunately been small to medium-sized events. Although small to mid-sized volcanic eruptions are less extreme events, they occur more frequently and provide a more regular stream of ash and gases to the environment than larger eruptions.

Volcanic aerosols can be external mixtures of ash, sulfates, and hydrometeors and/or internal mixtures of ash coated with sulfates, water, and/or ice [7]. Ash and sulfates are considered the dominant aerosol components of most eruptive plumes (e.g., [8]). In volcanic eruptions,

http://dx.doi.org/10.5772/63421

sulfates are formed from a reaction between emitted volcanic sulfur dioxide (SO_2) and water and can remain in the stratosphere for up to 3 years [9], causing cooling at the surface and warming in the stratosphere [10]. The lifetime of fine ash (aerodynamic diameter <2.5 μm) in the stratosphere is on the order of a few weeks [11]. Consequently, sulfates are usually the only aerosol included in global climate perturbation estimates from a particular eruption [12]. However, volcanic ash and sulfate aerosols in the troposphere are important on a regional level and have comparable lifetimes (approximately days to weeks). Therefore, both ash and sulfate must be included in assessing the regional radiative impact of volcanic aerosol.

Volcanic aerosols can reflect and absorb shortwave (SW) radiation, and they scatter, absorb, and emit radiation in the longwave (LW) part of the spectrum. The interaction of volcanic aerosols with electromagnetic radiation can cause warming or cooling of the surface and atmosphere depending on the reflectivity of the underlying surface, the solar zenith angle (SZA), the optical properties of the aerosol layer, the vertical structure of temperature and humidity, and cloud characteristics. Ash deposits can lower the albedo of highly reflective snow and ice surfaces and may perturb the Arctic radiation budget and cause early snowmelt, analogous to dust deposits [13] and soot deposits [14]. Little consideration has been given to the radiative impacts due to volcanic ash deposits in snow (e.g., [15, 16]), and even fewer studies focus on the surface radiative impacts of volcanic ash deposits from Arctic eruptions or map the entire extent of the deposit area (e.g., [17, 18]). Additionally, ash [19, 20] and sulfates [21] can serve as cloud condensation nuclei and ice nuclei. **Figure 1** illustrates the broad impacts volcanic aerosols can have on the Arctic environment.

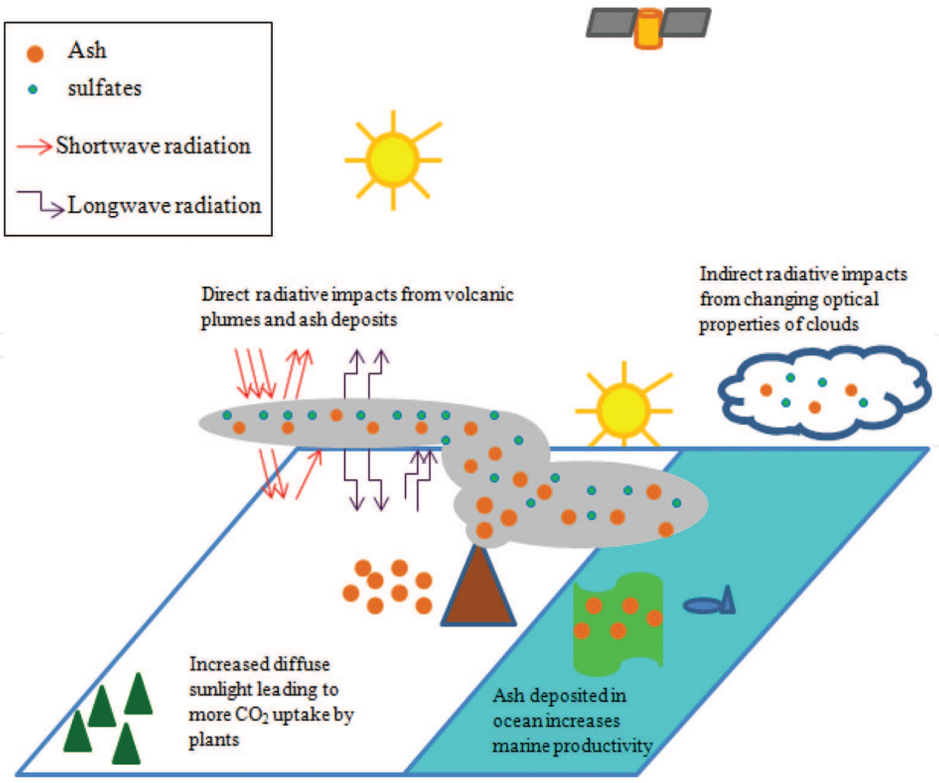

Figure 1. Broad impacts of volcanic aerosols on the Arctic environment.

This chapter will review the current state of the science behind the radiative impacts of volcanic aerosol in the Arctic and what remains to be explored. The work will touch on techniques involving satellite remote sensing, field measurements, and different types of modeling (radiative transfer, ash dispersion and transport, and atmospheric chemistry and circulation) that are used to help constrain the complexities of this problem. This chapter will focus mainly on the direct radiative impacts and then will briefly touch on other effects volcanic aerosols can have on the Arctic environment.

2. Radiative impacts of volcanic aerosol plumes

Determining the radiative influence volcanic aerosols have on the Arctic environment is a challenging problem because of the complexities of volcanic aerosols and the few measurements of their physical, optical, and chemical properties, which must be known to calculate radiative transfer and spectral refractive index. Particle counters on balloons and aircrafts have measured size distributions of stratospheric sulfate aerosol several weeks to months after an eruption (e.g., [22]), but these measurements are not helpful in determining the size distributions of less aged plumes of sulfate and/or ash. Models have been developed that include the sulfate formation and aging process [23] and have been added into general circulation models (GCMs) [11]. Size distributions for volcanic ash are dangerous to measure in situ and are usually measured on ash fall samples, which are not representative of atmospheric size distributions because of sorting that takes place during transport [24]. The role of plume aging on altering the composition and size distribution of volcanic aerosol is important to consider and is expected to substantially influence the radiative impacts.

In addition to SZA, surface albedo, and optical properties of aerosol, there are more aerosol layer-specific characteristics that must be known for radiative calculations. For an aerosol plume, these include aerosol optical depth (AOD), physical thickness, and vertical placement of the layer in the atmosphere. Sun photometers and ground-based lidars can help determine AOD, and ground-based lidars can also be used to obtain thickness and vertical placement. However, the coverage of ground-based sensors is limited. Due to the limitations of ground-based sensors and field measurements as well as the remote locations of Arctic volcanoes, satellite remote sensing is essential for monitoring aerosol from volcanic eruptions. The NASA afternoon satellite constellation A-Train provides a unique opportunity to examine eruptions and the evolution of volcanic plumes. The A-Train consists of six polar orbiting satellites [Aqua, Aura, Cloud-Aerosol Lidar and Infrared Pathfinder Satellite Observations (CALIPSO), CloudSat, GCOM-W1, and OCO-2] flying in close configuration, each equipped with different sensors measuring in wavelength ranges from the ultraviolet (UV) to radio. Combining the data retrieved from several sensors allows for an unprecedented view of volcanic eruptive plumes.

The Moderate Resolution Imaging Spectroradiometer (MODIS) instrument flying aboard Aqua and Terra satellites, the Ozone Monitoring Instrument (OMI) on the Aura spacecraft, and the Cloud-Aerosol with Orthogonal Polarization (CALIOP) aboard the CALIPSO platform are sensors capable of detecting volcanic aerosols. The MODIS instrument provides true color

http://dx.doi.org/10.5772/63421

images of ash plumes and deposits and AOD of volcanic plumes. The OMI provides a UV aerosol index (AI) that can detect the presence of UV-absorbing aerosols, such as ash, dust, smoke, and SO_2 emissions. CALIPSO provides the vertical plume structure, which is useful in determining the placement of the plume in the atmosphere, the plume top height, and the plume thickness. In addition to these platforms, the Atmospheric Infrared Sounder (AIRS) aboard the NASA Aqua satellite views the Earth in the infrared (IR) and is sensitive to the SO_2 absorption band at ~7.3 μm [25]. AIRS and OMI observations can often complement each other, as AIRS is not dependent on solar UV and OMI is less sensitive to water vapor, which hinders AIRS observations near the tropopause. However, in the Arctic, environmental conditions, such as meteorological clouds, little to no winter daylight, and high surface reflectivities, often hamper retrievals for passive instruments measuring in the visible and UV, such as MODIS and OMI, as well as space-based lidars, such as CALIPSO. It is because of these challenging environmental conditions that modeling of the eruptive plume transport, dynamics, and dispersion is essential to accompany, and sometimes supplement, satellite data retrievals in the Arctic region.

2.1. Tracking volcanic plumes

Tracking the movement, areal extent, and evolution of volcanic plumes is not only relevant for radiative purposes but also from an aviation safety and public health standpoint. It is possible to track both gaseous and particulate species in the volcanic plume using satellite remote sensing and transport modeling. Two of the most common volcanic gases, H_2O and CO_2, are also major atmospheric constituents, making them hard to distinguish from the background. Volcanic SO_2, however, has a relatively low background concentration, making it an ideal trace gas for many volcanic eruptions. SO_2 is observable in both the UV and thermal IR (TIR). For use as a tracer in Arctic environments, the absorption bands in both the UV and TIR are critical. During the Arctic winter, the lack of daylight hinders UV observations, as solar radiation is the dominant source of UV, whereas TIR measurements can still be collected. Conversely, low thermal contrast between the volcanic plume and the ambient environment makes observations in the TIR difficult, diminishing the potential for TIR instruments to observer older, cooler plumes. Due to the strong absorption of water in the TIR, high water vapor content in the lower troposphere can also limit TIR observations of SO_2 [25]. In most of the world, this means that TIR instruments are best used to observe plumes above 3 km [25]; however, the generally low relative humidity in the Arctic can mitigate this issue.

A combination of plume observations from both UV and TIR observations can allow plumes to be tracked for days or even weeks depending on the size of the eruption. As a volcanic plume matures and moves away from its source, dilution from atmospheric mixing and conversion of SO_2 to sulfate aerosol make plumes more difficult to separate from the surrounding atmosphere. Atmospheric models, such as NOAA HYSPLIT [26, 27], which predict the direction and altitude of the plume movement, can complement the use of AIRS, CALIPSO, MODIS, and OMI data to improve and prolong plume tracking metrics.

Tracking both Arctic and sub-Arctic plumes is crucial, as even plumes in the sub-Arctic region can be easily transported into the Arctic, possibly amplifying their environmental impacts in

this sensitive region. SO_2 from the initial activity from the 2012 to 2013 eruption of Plosky Tolbachik Volcano, in the Kamchatka Peninsula, could be observed for a week as it moved northwest from the source and then across the Siberian Sea before heading south again [28]. Despite its longevity, the Plosky Tolbachik plume had remarkably little influence on the Arctic environment because it was predominately transported in the troposphere, over water, during the winter, and had significantly more SO_2 than ash [28, 29].

Due to the lower neutral buoyancy height of particles versus that of gases and the possibility of wind shears, particles may be concentrated at lower levels in the atmosphere and can move in different directions than the gases. Tracking ash in volcanic plumes can be accomplished with the use of UV and visible satellite remote sensing (e.g., OMI AI and MODIS AOD) as well as using IR brightness temperature difference (BTD) techniques (e.g., [30, 31]), employing instruments such as AIRS, Geostationary Operational Environment Satellite (GOES), Advanced Very High Resolution Radiometer (AVHRR), and MODIS. Often called the "split window technique," this method takes advantage of the distinctive negative BTDs that result from volcanic ash/sulfates in bands centered at 11 and 12 μm and can be used to estimate optical depth, particle sizes, and masses of ash/sulfate that match the observed BTD from varying these parameters in a radiative transfer model [30]. This method assumes spherical particle shapes, a thin plume parallel to a homogenous surface, and a predetermined range of particle sizes. Fixed refractive indices are often used (selection of these are described further in Section 2.2), but the sensitivity as demonstrated by Wen and Rose [30] is higher for the assumed size distribution than the refractive indices. Meteorological clouds can give similar BTD values to ash and sulfate, and the BTD must be used along with other information (e.g., true color images) to support a definitive particle detection. Dense eruptive plumes can cause issues for the retrieval algorithm, since it was developed for a semitransparent plume, and are better suited for single-band studies. Positive BTDs have been used to infer the presence of ice in the eruptive plume, and similar radiative transfer calculations were done to estimate the size distributions and masses of ice [31]. However, ice is often not the dominant particle in eruptions that occur above 40°latitude, in contrast to those that occur closer to the tropics, because the entrained tropospheric air has a lower water vapor content at higher latitudes [7]. Particle depolarization ratios from CALIPSO may also be used to confirm the presence of nonspherical particles within the plume, but lidars are more suited to studying plume profiles than areal extents. Ash transport models are another tool for understanding plume transport and ash deposition and are discussed later in this chapter (Section 3.1).

2.2. Constraining the optical properties of volcanic plumes

To develop a microphysical model, the compositional types of volcanic aerosols present in the eruptive plume and their refractive indices, size distributions, and relative abundances with respect to other aerosol types present must be ascertained. Refractive indices can be measured in a laboratory for a variety of aerosol types and compositions. The Optical Properties of Aerosols and Clouds (OPAC) data set [32] compiles refractive indices for several typical aerosols under different atmospheric humidity conditions. To represent volcanic sulfate, sulfuric acid solutions of ~70% are often used (e.g., [12]), but at Arctic ambient air temperature

and relative humidity these concentrations tend to be lower (~40–50%) [33]. Because the temperature and relative humidity in a fresh volcanic plume are higher than that of the surrounding air, sulfuric acid solutions closer to 70% are a more realistic estimate for a fresh volcanic plume than the ambient air mixtures. The refractive indices of ashes with varying silica content have also been measured (e.g., [34]) and are commonly used to represent an ash component in microphysical models.

Other quantities that must be included in the microphysical model (i.e., size distributions and relative abundances) cannot be measured directly, especially in the case of "fresh" plumes. Most microphysical models treat volcanic aerosols with a lognormal size distribution, similar to the form from Kearney and Watson [35]:

$$n_c(r) = \frac{1}{\sqrt{2\pi\sigma}} e^{-\frac{(\ln(r)-\mu)^2}{2\sigma^2}} \tag{1}$$

where n_c is the particle number concentration, r is the particle radius, and σ is the variance of the size distribution or the log of the standard deviation:

$$\mu = (\ln \text{Reff}) - 2.5\sigma^2 \tag{2}$$

where Reff is the effective radius [35].

Sulfates are typically nanometer-scale particles and occur only in the fine-mode fraction (aerodynamic diameter <2.5 μm), but ash sizes can vary greatly from coarse to fine. As the plume ages, sulfate aerosols grow larger in size and more numerous, as the effective radius for ash becomes smaller and larger grain sizes are scavenged. A more sophisticated model, such as a GCM, may be able to estimate and track the evolution of size distributions and the relative abundances of the aerosol types given a set of initial conditions and may even treat sulfate formation from SO_2 [11]. However, these estimates are difficult to validate and initial conditions may add uncertainty, especially in the Arctic. When available, satellite data may be used to deduce size distributions (e.g., [30]), and ratios of fine- and coarse-mode aerosols can be constrained to determine the proper proportions to externally mix aerosol types (e.g., using MODIS fine-mode fraction retrievals). Literature investigations of size distributions for representative eruptions can be used to study end-member cases of fresh and aged plumes under Arctic conditions [29, 35].

An additional consideration when determining the optical properties of volcanic aerosol is whether to consider particle nonsphericity of ash and ice in the calculations. This can be done employing the T-matrix method. However, because the relative errors in radiative flux calculations for using the single scattering properties of spherical particles to approximate those of nonspherical dust particles are low [36], optical properties calculated with the Mie theory are often still used.

2.3. Comparing the radiative impacts of Arctic aerosol plumes

The direct aerosol radiative forcing (DARF) of two moderately thin volcanic layers from a mid-sized volcanic eruption have been compared to those for other aerosol types [29]. Two volcanic layers were chosen to represent a young, ash-rich/sulfate-poor plume and an older, sulfate-rich/ash-poor plume. Radiative modeling was used to obtain upward and downward fluxes. Net fluxes (Fnet) for both the SW and LW components at the top of the atmosphere (TOA) and at the surface were computed by subtracting the upward flux from the downward flux. The total net flux at TOA and at the surface were then calculated by adding the respective SW and LW net fluxes. DARF efficiency (DARFE), defined as the change in the net flux with respect to the change in AOD (550 nm), was computed as

$$DARFE = \frac{\Delta F_{net}}{\Delta AOD_{550\ \mathrm{nm}}} \tag{3}$$

To calculate DARFE for an aerosol layer, the surface DARFE was subtracted from the DARFE at TOA. The units of DARFE are W m^{-2} AOD^{-1}, and a similar definition of DARFE to that of Stone et al. [1] was selected to consistently compare radiative impacts for all aerosol types. Calculations of DARF were done by multiplying DARFE by the layer AOD, resulting in units of W m^{-2}.

Volcanic eruptions are special events because of their ability to create aerosol layers many times thicker and more optically opaque than sources of other aerosol types frequently found in the region. In considering the nature of volcanic eruptions, it is expected that they could produce larger vertical loadings and dominate over the radiative impacts of other aerosols. Although many factors influence the regional radiative impacts, similar surface albedo, AOD, SZA, and plume thickness for each aerosol type were chosen to study the effects of different aerosol compositions and size distributions alone (for more information, see Table 4 in Young et al. [29]). A comparison of DARFs for two volcanic aerosol compositions [29], mineral dust

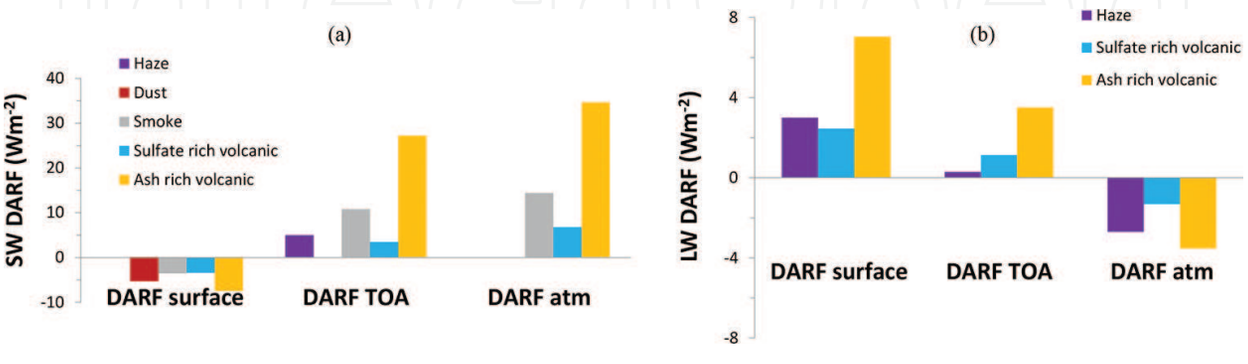

Figure 2. (a) SW DARFs [37], dust [2], smoke [1], and ash- and sulfate-rich volcanic aerosols [29]. Values of forcing for dust were only available at the surface. (b) LW DARFs for haze [38] and ash- and sulfate-rich volcanic aerosols (taken from Young et al. [29]).

[2], wildfire smoke [1], and haze [37, 38] is presented in **Figure 2** (taken from Young et al. [29]).

The ash-rich volcanic mixture, followed by mineral dust, attenuates the most incoming solar radiation at the surface and also absorbs more solar radiation in the layer than the other aerosol types (**Figure 2a**). The ash-rich mixture is the most important aerosol type with regards to the LW radiative impacts (**Figure 2b**). It should be noted that the LW forcing for smoke is negligible due to small particle sizes [39] and is not shown in **Figure 2b**. LW forcings of dust and volcanic aerosols are important because those particles are of sufficient size to interact with LW radiation. In the Arctic, LW radiation can dominate the forcing during seasons when the sun is low and can change the sign of the total forcing, but the LW component is rarely considered in radiative assessments of Arctic aerosols. Comparisons of both SW and LW components suggest that a thin ash-rich volcanic layer can dominate the aerosol radiative impacts in the Arctic.

3. Radiative impacts of volcanic deposits

Similar information to plume radiative modeling is needed to calculate the radiative impacts of ash deposited onto ice and snow, but knowledge on ash deposit loadings and areal extents also must be ascertained. Ground measurements are helpful but usually do not map out the entire extent of deposits or provide an adequate spatial resolution of samples. Volcanic ash transport models can assist in characterizing ash plumes and deposits. Past research has employed GCMs to simulate the dispersion and deposition of volcanic ash by assigning an initial flux amount of ash into the atmosphere (e.g., [11]) without treating the source conditions of the eruption (e.g., the initial distribution of ash in the eruptive column). Failing to consider the dynamics of the eruption and initial eruptive column will impact the regional transport and deposition of ash. In efforts to account for previously neglected eruption dynamics, a preprocessing tool was developed to determine the initial ash fields from source conditions for input into mesoscale atmospheric chemistry models [40]. As an alternative to GCMs, volcanic ash transport and dispersion models (VATDMs) compute initial ash fields directly from eruption source condition input parameters, consider a full-sized spectrum of ash, and can include nonspherical ash particles.

3.1. Constraining VATDMs

VATDMs can be presented in either Eulerian (e.g., Fall3D and TEPHRA) or Lagrangian (e.g., Puff and HYSPLIT for volcanic ash) reference frames. Volcanic advection-diffusion models (e.g., [41]) are Eulerian models that can predict atmospheric ash concentrations and ground deposit loadings by considering advection, turbulent diffusion, and gravitational settling, making them useful tools in assessments of the radiative impacts of ash deposits. In general, advection-diffusion models require input of source conditions [mass flow rate (MFR), source type, and plume temperature], ash properties (initial size distribution, particle density, and shape), and transport conditions (meteorological data and diffusion coefficients).

Commonly, MFR is estimated by comparing eruption plume heights to those predicted with simple plume theory for a particular eruption rate (e.g., [42]), assuming there are no variations in plume height during the eruptive activity. Error can be introduced when determining the height of the plume, which is often deduced from seismic data or reported by pilots in the area. Another technique that is often used involves erupted masses determined from mapped deposits and the seismic durations of eruptive events [43, 44], but this technique relies on the assumption that MFR is constant over the entire duration of the eruptive episode. The success of this method hinges upon a thorough and timely sampling of the eruptive deposits, including only ash deposited from the relevant eruptive event. Because of the large uncertainties that go into any MFR calculation, independent estimates of MFR for a given eruptive event can vary over orders of magnitude [43–45]. There are not many good estimates of MFR for Arctic eruptions due to the remote locations of many volcanoes, making MFR a poorly constrained parameter to which advection-diffusion models can exhibit a high degree of sensitivity [46].

The volcanic column source type determines how ash concentrations will be initially allocated within the atmosphere. For example, the Fall3D model [41] handles three different source types: plume, point, and Suzuki. The plume source describes the distribution of ash within a rising, hot, buoyant plume in which ash concentrations increase with height, up to a height of neutral buoyancy with the atmosphere. The point source dispenses all ash from a single point and height within the atmosphere. The Suzuki source allows for the height of the largest ash concentration and how the total mass is distributed around it to be chosen based on the strength of the eruption (i.e., more violent eruptions distribute the highest concentration of ash more closely to the maximum column height).

Due to the dangers involved with measuring the size distributions of ash in plumes in situ, the initial size distributions used in VATDMs are measured from deposits in the field. These measurements are often depleted in fine ash because fine particles can be swept to great distances from the volcano, where they cannot be collected and measured [47]. Particle densities and shapes are also typically measured from field deposits and, along with the size, also affect the settling rate of ash. Particle density varies with vesicularity, which can be a function of particle size, and particle shapes can range widely from spherical to nonspherical [48]. Advection-diffusion models, such as Fall3D, can exhibit high sensitivity to particle shape [46], which is a parameter that eruption-specific and extensive field deposit sampling could better constrain relatively easily.

Transport-related parameters (i.e., wind fields and diffusion coefficients) govern the advection and diffusion portions of the model. The diffusion coefficients represent the dispersion of ash due to small-scale turbulent motion without directly modeling the scale of this process and impact the width of ash plumes and deposits [41, 49]. The values of diffusion coefficients can be challenging to determine and are often tuned to match model results with observations, thereby accounting for some turbulent processes that are not directly modeled. Most of the transport processes for large eruptive columns occur outside the boundary layer, causing the vertical diffusion coefficient to be negligible compared to the horizontal diffusion coefficient [49]. Despite the uncertainty and wide range of possible horizontal diffusion coefficients, the

model is typically not as sensitive to this parameter as it is MFR, some source types, and particle shape [46].

To constrain VATDMs in the Arctic, where data are sparse, Young et al. [46] developed a methodology to use the most data-rich event and obtain the best-fit model parameters by solving the inverse problem [46]. These best-fit parameters were then used to extrapolate those for other less studied eruptive episodes. This methodology was applied by Young et al. [46] to the 2009 eruption of Redoubt Volcano in Alaska, USA, and would be applicable to other eruptions for which a small period of the explosive activity was better characterized than most of the explosive events. Although this technique resulted in good to moderate model agreement with the available satellite and field data, the model had particular difficulty reproducing ash deposit loadings measured by Schaefer and Wallace (2012) in the far field (200–300 km from the vent) for even the most studied eruptive episode [50]. Other works employing Eulerian models to simulate ash deposition from the same eruptive event had similar issues for many model runs in the far field using a similar model set-up [44, 51]. Potential sources of error for all studies include distinguishing between ash layers from different eruptive events in the field [43], issues with wind field resolution through high elevation regions, and ash aggregation effects (discussed below in detail) that are not currently treated by any volcanic transport model.

Aggregation models, such as the one developed by Telling et al. [52], should be incorporated in VATDMs. Additionally, the process of comminution, which is the break-up of particles due to collisions, is not considered. Comminution is likely important in the initial conduit, where particle densities and energies are high and more bounce events between particles occur than aggregation events [53] and also, potentially, in the lowest region of the volcanic column, where particle densities are highest. Aggregation is more critical to consider when attempting to reconcile deposition and long-range atmospheric transport models with field and satellite data.

3.2. Ash aggregation studies for future VATDM improvements

Aggregation, or sticking, between volcanic particulate is a key source of error in any volcanic transport model. Volcanic ash is defined as any solid particulate with a diameter less than 2 mm in size [24]. Depending on the eruption type, size, and duration, fine ash (1–10 μm) typically has a lifetime on the order of days [11, 54], whereas fine ash (0.1–1 μm) can remain in the atmosphere for months to years in the case of stratospheric eruptions [11]. This can be a particular concern for Arctic eruptions because the boundary between the troposphere and stratosphere is lower in the Arctic environment. Typically, the Arctic tropopause occurs between 8 and 10 km, depending on season, whereas the tropopause occurs between 12 and 16 km over the tropics.

Marzano et al. [55] cited the lack of information regarding particle aggregation as a key source of error in their efforts to model the 2004 eruption of Grimsvötn. More recently, the 2010 eruption of Eyjafjallajökull, Iceland, produced an abundance of both fine ash (raising concerns for aircraft travel and respiratory health impacts) and coarse ash [54]. However, aggregation processes ultimately removed much of the fine ash close to Eyjafjallajökull, dampening the

regional hazards [56] and demonstrating the importance of these processes on both regional and global scales [19, 56].

Gilbert and Lane [57] provided a number of classifications for aggregates, but the two broadest categorizations are simply dry and wet. Dry aggregates are bound by particle charging [57], which can be a result of either triboelectric charging, resulting from particle-particle interactions in the flow, or fractoemission, which occurs in the conduit during fragmentation [58]. Wet aggregation arises from the presence of water in a volcanic flow, forming when liquid-coated particles collide and stick together or when dry aggregates are scavenged by a water droplet [57]. In general, the Arctic environment is drier than that in the mid-latitudes and tropics, and this is particularly true in the winter over land. Consequently, electrostatic aggregation is a particularly important consideration in the Arctic, although wet aggregation is still likely dominant in a fresh eruptive plume because water is abundant and atmospheric mixing has not yet cooled the plume.

Numerous models have been proposed to treat aggregation in volcanic and atmospheric simulations. The most simplistic of these typically assume that a certain percentage of ash will aggregate, that only wet or dry aggregation processes are important but not both [19], or that particle aggregation will mimic water droplet coalescence. More complex formulations treat aggregation as a function of Stokes number, with aggregation efficiency decreasing as the Stokes number increases [59]; however, this accounts only for wet aggregation. This is a serious shortcoming for any model used in an Arctic setting because the environment over land is typically dry, especially in winter, and aggregation processes would be poorly modeled as soon as the volcanic plume began to dilute. Research has also been done to experimentally determine how much water is needed to promote wet, over dry, aggregation [52, 57] and to determine the degree of charging required to form electrostatic aggregates [52, 58]. The delineation between wet and dry aggregation zones occurs at ~71% relative humidity [20, 52] and the wet and dry aggregation zones, which each have different behavioral characteristics, can be defined accordingly. Telling et al. [52] developed these experimental relationships into a series of equations that define aggregation efficiency as a function of the collisional energy of two particles for the wet and dry cases separately.

Considering aggregation in radiative calculations would call for an updated microphysical model of ash, which is discussed by Textor et al. [19]. In both dry and wet cases, aggregation would influence how the size distribution evolves with time. The formation of heavier aggregates from smaller particles would lead to aggregates with different shapes than the individual particles and change the gravitational settling rates of ash. Wet aggregation involves the addition of a water layer, which could also be frozen into an ice layer and would modify the refractive index of the ash.

3.3. Constraining a radiative model for volcanic ash deposits

Radiative modeling of volcanic ash deposits on snow and ice requires some similar knowledge to that of plume modeling (i.e., SZA, underlying surface reflectance, ash effective radius, and refractive index) but also must include additional snow layer properties (i.e., snow layer thickness, snow density for each layer, and snow effective radius) and particle mass mixing

http://dx.doi.org/10.5772/63421

ratios of ash in snow. A spectral or monochromatic underlying surface reflectivity can be used, but the model would not be sensitive to this parameter if the snow depth is large.

Even the most detailed depositional maps are often not resolved enough to study the radiative impacts due to the entire extent of the deposit, especially in the aerosol size range (radius ≤50 μm), because the measured area typically includes only deposits proximal to the vent. Modeled depositional loading fields can be converted into mixing ratios using the density of snow and the mixing depth of ash in the snowpack. As reported by Young et al. [46], the shape of the ash particles is important in advection-diffusion modeling, with spherical particles having better agreement with field measurements in most areas, whereas nonspherical particles produce loadings that agree better with field data for locations ≥210 km from the vent [46]. Advection-diffusion models can also do fairly well at reproducing deposited ash median radius compared to field data (except in areas ≤12 km from the vent, where aerosol-sized particles are less abundant), which is useful for optics calculations [18].

Assuming only aerosol-sized ash particles are being considered, the optical properties of the ash may be calculated with the Mie theory for a lognormal size distribution and deposited ash mean effective radii and standard deviation fields determined from transport modeling. This assumption can be made because the larger particles are relatively low in abundance and are concentrated in regions close to the vent [43]. Ash refractive indices for a given composition can be taken from previous laboratory studies, where available (e.g., [34]). Although the inclusion of nonspherical particles is important for transport modeling [46], spherical particles and the Mie theory may be used in calculating the optical properties of ash because relatively little error arises from approximating particles as equal volume to projected area spheres in the radiative flux calculations [17, 36].

The snow properties required by the radiative model can be measured in the field, but in the absence of field data and adequate spatial/temporal coverage data sets, such as the Natural Resources Conservation Service (NRCS) Snow Telemetry (SNOTEL), may be used to estimate snow layer thickness and density. The refractive indices of ice are often taken from the literature (e.g., [60]). Snow effective grain size radius can vary between 50 and 1100 μm (e.g., [61]), with new snow having smaller grains. If snow effective radius profiles are unknown for the time and region of interest, smaller grain sizes may be used to represent fresher snow and larger sizes for older snow.

At the time of eruption, ash would be deposited on top of the snowpack, which could be blanketed by snowfall or another ash layer [62]. The covering of ash deposits with new snow may substantially increase the surface albedo, and the layering structure of snow and ash should be considered. It is likely that measurements of this kind have not been made throughout the entire extent of the ash deposits, and a representative layering scheme may need to be constructed from what is known. However, new snowfall onto ash may not have a long-lived effect on albedo because, as the snow melts, water will flow downward through pore spaces in the snow, and ash will become concentrated at the top of the snowpack. A concern might also be blowing winds spreading freshly fallen ash, but after melting starts wet ash particles will stick to the snow.

3.4. Radiative impacts of aerosol deposits in the Arctic

The radiative impacts of several types of aerosol deposits (i.e., black carbon, volcanic ash, and dust) in snow measured in the field are compared to those for volcanic ash deposits from the mid-sized 2009 eruption of Redoubt Volcano, modeled by Young et al. [18]. High surface reflectivity and cloudy conditions prevented the retrieval of satellite albedos for this eruption, and there were also no known measurements of albedo in the field, both of which are typical issues surrounding Arctic eruptions. In keeping with isolated observations of complete ash cover in many regions, significant albedo reductions were modeled for these areas [18]. **Table 1** breaks down the particulate species and the quantities compared by Young et al. [18].

Aerosol species	Reference	Loadings (ppb)	Percent surface albedo reduction	SW surface forcing (W m^{-2})	Percent increase in melt rate compared to pure snow
Ash[a]	Young et al. [18]	7×10^{4}–1×10^{8}	0–85	0–96	220–330
Ash[b]	Young et al. [18]	≤1.6×10^{7}	X	X	140–160
Black carbon	Clarke and Noone [62]	5–50	1–3	X	X
Dust	Skiles et al. [64]	2×10^{5}–4×10^{6}	X	35–70	X
Ash	Dadic et al. [16]	1×10^{0}–1×10^{6}	0–37	X	X
Ash	Driedger [15]	X	X	X	≥90

Please note that due to the nature of the measured deposits not all of the quantities are directly comparable (as will be discussed in the text) but are presented here to illustrate the extents of impacts possible from various particles. Calculations were done for a layer deposited on both new and old snow, and the ranges reported for albedo reduction and forcing include both cases from the edges of the deposits to the vent [18]. Melt rate increases were calculated at the maximum loadings only to report an upper bound. Information that was not reported is denoted by an X.
a Ash layer covering loadings from the vent to the edges of the deposits.
b Ash layer calculations only considering low to intermediate loadings.

Table 1. Measured radiative impacts of black carbon, volcanic ash, and dust deposits on snow compared to those modeled by Young et al. [18] for volcanic ash.

For a similar particle size and concentration, black carbon is far more absorbing than ash [63], but at the large loadings that may be produced by a mid-sized eruption ash would cause the most significant albedo reductions. To compare volcanic eruptions, it is important to look at albedo changes from similar loadings. The greatest deposit loading used in Young et al. [18] is two orders of magnitude larger than that measured by Dadic et al. [16] in Antarctica. It is

possible that the deposits measured by Dadic et al. [16] were from a smaller eruption (or a mid-sized to large eruption under windier conditions), the study had only measured ash in more distal locations, or greater mixing of ash and snow had taken place. Young et al. [18] reported an albedo reduction of ~37% for ash deposited on new snow when considering only loadings at more distal locations (~200 km from the vent) and concentrations of ~2.8×10^7 ppb [18]. This albedo reduction is comparable to that of Dadic et al. [16] for the area of the largest ash concentration measured. These studies may not be directly comparable, however, due to potentially different size distributions in deposits at the locations of interest.

The SW surface net fluxes calculated by Young et al. [18] were made at a daily mean SZA for late March and can be viewed as 12-hour daily averages [18]. Skiles et al. [64] also computed springtime daily mean forcings for dust deposits on snow in Colorado. The SW imaginary part of the refractive index for ash [34] is similar to that of dust [65], but the mean daily forcings from dust would be much smaller in the Arctic than in Colorado. This is because the average Arctic dust concentrations are about two to three orders of magnitude lower (i.e., [66]), and the incident solar radiation is lessened at higher latitudes. Using the method of Skiles et al. [64] to calculate minimum forcings due to the direct effects of ash deposition onto snow alone, Young et al. [18] computed a range from the edges of the deposit to the vent of ~0 to 96 W m^{-2}.

The restricted degree-day radiation balance approach described in Melloh [67] was used by Young et al. [18] to estimate a range of melt rates from SW surface net fluxes. Although no significant increases in melt rate were found for the edges of the deposits, regions with larger ash loadings had daily melt rates that were substantially greater than pure snow (~220–320%). However, these areas included ash layer thicknesses exceeding 0.3 cm, which will start to insulate the snow at this thickness [15], making these estimates of snowmelt an upper bound. Considering only intermediate loadings ≤1.6×10^7 ppb with layer thicknesses <0.3 cm achieved more conservative maximum melt rates ~140% to 160% larger than ash-free snow. These estimates are generally in agreement with conservative maximum snowmelt increases of at least 90% measured for snow plots manually covered with ash by Driedger [15]. Melting in regions where snow is present year-round can lead to an increase in albedo that results in further snowmelt. In areas that typically melt in the summer, early or accelerated snowmelts have the capacity to reduce runoff in later months and deplete water resources [68].

4. Other impacts

4.1. Indirect radiative effects

The indirect aerosol effect refers to the ability of aerosols to cause radiative perturbations by altering the microphysical properties (e.g., changing the refractive index, particle number, and/or size distribution), lifetime, and coverage of meteorological clouds, thereby also influencing the hydrological cycle [69]. The Intergovernmental Panel on Climate Change (IPCC) reports that the current understanding of the indirect effects of aerosols on clouds is low [70]. Studies have shown that sulfate from the eruption of Mount Pinatubo in the Philippines produced a global impact on cirrus formation and evolution [21] through increases in aerosol number,

homogeneous ice nucleation rate and ice crystal number, and ice water path [21, 71]. Additionally, it was found that ash can uptake water efficiently and can serve as cloud condensation nuclei [20] and ice nuclei [19]. The indirect effects in the Arctic may be different than in other regions because of the special properties of the surface and atmosphere, and the Arctic is more sensitive to aerosol effects [69]. The aerosol indirect effects due to volcanic eruptions may be particularly significant, as eruptions supply a large number of particles (i.e., ash, ice, and sulfates) compared to the low particle levels in the ambient Arctic atmosphere. More research is needed on the subject of the indirect radiative effects of volcanic aerosols in the Arctic.

4.2. Effects on ecosystems

The effect that volcanic eruptions have on ecosystems has been well documented. Forests [72], oceans [73–75], and even large global cycles, such as CO_2 variability typically controlled by the El Niño-Southern Oscillation (ENSO) [76, 77], can be influenced by volcanic eruptions. This section examines a few of these effects in further detail.

4.2.1. Increased diffuse radiation to plants

Beyond the direct radiative impacts of volcanic eruptions, volcanic ash and aerosol can have long-lasting secondary effects. The ash-rich eruption of Tambora Volcano, Indonesia, in 1815, resulted in the well-known "year without summer" in 1816 [78]. Stratospheric ash loading reduced direct solar radiation globally, leading to widespread cooling, crop failure, and slowed forest growth [72, 78]. However, Gu et al. [79] found that large aerosol-rich eruptions, such as Mount Pinatubo, can have a quite different effect. Although the 1991 eruption of Mount Pinatubo did decrease the direct solar radiation as expected, it also increased the diffuse solar radiation [79]. Gu et al. [79] showed that this increase in diffuse solar radiation led to an increase in forest photosynthesis, which, in turn, led to a temporary decline in the amount of atmospheric CO_2 [76]. Although neither of these eruptions occurred in the Arctic, both the Tambora and Mount Pinatubo events were felt globally for years afterward [69, 79] and potentially had a disproportionate effect on the Arctic environment either by promoting additional growth of vegetation in the tundra or by reducing the already short Arctic growing season. Further study is needed to better understand the effects of large volcanic eruptions on the Arctic environment, which is home to thousands of plant species.

4.2.2. Increased ocean productivity

Plate tectonics dictate that many of Earth's explosive volcanism sources are located near oceans and the effects of volcanic eruptions on ocean ecosystems have only been examined in a few studies. Olgun et al. [80] found that eruptions from Mount Etna, Italy, have contributed appreciable amounts of nitrogen, phosphorus, silicon, iron, and zinc to the Mediterranean Ocean between 2001 and 2007. Durant et al. [75] found enhanced amounts of calcium, sodium, and iron in lakes following the 2008 eruption of Chaitén Volcano, Chile. The iron contribution, in particular, made by volcanic deposits, has been particularly interesting to studies of ocean chemistry. Much of the ocean away from continental boundary regions is iron poor [73]. Deposits of volcanic ash, which becomes coated in minerals, deliver iron, a necessary nutrient

for phytoplankton [73, 74], to otherwise iron-poor regions of the ocean. Phytoplankton blooms were noted after the 2008 eruption of Kasatochi Volcano (Alaska) [74], Mount Spurr (Alaska), Arenal Volcano (Costa Rica), and Sakurajima Volcano (Japan) [73]. The phytoplankton blooms were large enough to be seen by MODIS from space [73, 74].

The effect on Earth's ecosystem does not end with increased phytoplankton growth, though. Similar to the effect seen in forests, the large phytoplankton blooms cause a temporary but significant decrease in atmospheric CO_2 [73, 81]. The decrease in CO_2 caused by moderate to large volcanic eruptions is on par with that caused by ENSO and can mitigate or exacerbate the effects of ENSO depending on when during the ENSO cycle an eruption occurs [76, 77]. Modeling studies by Rothenberg et al. [81] and Frölicher et al. [77] both showed that the additional CO_2 uptake results in further global cooling that is particularly strong in the Arctic region.

5. Conclusions

Volcanic aerosol, although sporadically present, can have a profound influence on the Arctic environment. There is a potential for volcanic aerosol to provide a sizeable contribution to the radiative effects and even exceed the impacts of other types of aerosol when significant amounts of volcanic ash are present, as in young volcanic plumes and volcanic ash deposits. The composition, thickness, and AOD of volcanic plumes vary greatly and are, in many cases, difficult to constrain. Meteorological clouds also often hamper satellite retrievals, making transport modeling necessary for plume tracking.

The development of multiphase models (e.g., [82]) to study eruption dynamics may assist in creating better microphysical models for volcanic ash and have the capacity to be modified to treat the formation and transport of other volcanic aerosols, such as sulfates and ice. The deployment of balloons with particle counters attached would also further our understanding of the evolution of aerosol size distributions in plumes, which are hazardous to fly through and difficult to fully characterize with deposit measurements. There is a need for better constrained eruption-specific model input parameters (i.e., MFR, source type, and nonsphericity of ash particles). Discrepancies in modeled and measured loadings tend to be larger farther from the vent, which could indicate issues with wind field resolution or aggregation and comminution processes. Existing aggregation models, such as the one developed by Telling et al. [52], should be incorporated in volcanic ash dispersion and transport models. Additionally, the process of comminution, which typically only occurs in the volcanic conduit, is not considered. These improvements to eruption source and dispersion parameters will provide more accurate ash deposition estimates, which are critical for understanding how volcanic plumes and deposits interact with the Arctic environment. Other plume-related simplifications, which are often made in radiative transfer modeling and which need to be addressed, include the partitioning of volcanic aerosol types at different altitudes and sulfate, water, and ice coatings on ash.

Loadings of ash and the optical properties of ash and snow are important to radiative calculations. Future studies should consider improving ash loading estimates and the acquisition of eruption-specific snow and ash properties for radiative modeling. The calculation of global radiative effects could be made possible by a more intimate coupling of volcanic eruption source conditions, transport, and deposition with radiative transfer and global circulation models. Improvements that could be made through fieldwork include measurements of albedo change and snow ablation rates, which could be done through coordination with local volcano observatories. Alternatively, laboratory simulations on a smaller scale could be conducted when fieldwork is not possible.

Additionally, volcanic aerosols may have strong impacts on ecosystems and the carbon cycle. Because of the important radiative effects of volcanic aerosols in the Arctic, it is recommended that volcanic aerosols be included in future assessments of the Arctic regional radiation budget to facilitate efforts in understanding the radiative impacts of natural aerosols on the Arctic environment. Because of the persistence of cloud cover in this region, the radiative impacts of meteorological clouds in the presence of volcanic plumes and deposits should be considered. The effects of volcanic aerosol on other permanently and seasonally snow-covered environments might also be considered; these include glaciers at lower latitudes (e.g., in the Andes) and in Antarctica.

Author details

Cindy L. Young[1*] and Jennifer W. Telling[2]

*Address all correspondence to: cindy.young@eas.gatech.edu

1 School of Earth and Atmospheric Sciences, Georgia Institute of Technology, Atlanta, GA, USA

2 National Center for Airborne Laser Mapping (NCALM), University of Houston, Houston, TX, USA

References

[1] Stone, R.S., Anderson, G.P., Shettle, E.P., Andrews, E., Loukachine, K., Dutton, E.G., Schaaf, C., Roman, M.O. Radiative impact of boreal smoke in the Arctic: Observed and modelled. J. Geophys. Res. Atmos. 2008;113(D14) pp. 1–17 . DOI: 10.1029/2007JD009657

[2] Stone, R.S., Anderson, G.P., Andrews, E., Dutton, E.G., Shettle, E.P. Incursions and radiative impact of Asian dust in northern Alaska. Geophys. Res. Lett. 2007;34:L14815. DOI: 10.1029/2007gl029878

[3] Simkin, T., Siebert, L. Volcanoes of the World. 2nd ed. Tucson: Geoscience Press; 1994. 369 pp.

[4] Thordarson, T., Self, S. Atmospheric and environmental effects of the 1783–1784 Laki eruption: A review and reassessment. J. Geophys. Res. 2003;108(D1):4011.

[5] Frogner-Kockum, P.C., Herbert, R.B., Gislason, S.R. A diverse ecosystem response to volcanic aerosols. Chem. Geol. 2006;231(1):57–66.

[6] Hildreth, W., Fierstein, J. The Novarupta-Katmai eruption of 1912: Largest eruption of the twentieth century. In: Centennial Perspectives. U.S. Department of the Interior, U.S. Geological Survey; 2012. Reston, Virginia USA, 259 pp.

[7] Rose, W.I., Bluth, G.J.S., Watson, I.M. Ice in volcanic clouds: When and where? In: Proceedings of the 2nd International Conference on Volcanic Ash and Aviation Safety. Washington, DC: OFCM, 2004.

[8] Andersson, S.M., Martinsson, B.G., Friberg, J., Brenninkmeijer, C.A.M., Rauthe-Schöch, A., Hermann, M., van Velthoven, P.F.J., Zahn, A. Composition and evolution of volcanic aerosol from eruptions of Kasatochi, Sarychev and Eyjafallajokull in 2008–2010 based on CARIBIC observations. Atmos. Chem. Phys. 2013;13(4):1781–1796.

[9] Carslaw, K.S., Boucher, O., Spracklen, D.V., Mann, G.W., Rae, J.G.L., Woodward, S., Kulmala, M. Atmospheric aerosols in the earth system: A review of interactions and feedbacks. Atmos. Chem. Phys. 2009;9:10087–11183.

[10] Robock, A. Volcanic eruptions and climate. Rev. Geophys. 2000;38:191–219.

[11] Niemeier, U., Timmreck, C., Graf, H.F., Kinne, S., Rast, S., Self, S. Initial fate of fine ash and sulphur from large volcanic eruptions. Atmos. Chem. Phys. 2009;9(22):9043–9057. DOI: 10.5194/acp-9-9043-2009

[12] Stenchikov, G.L., Kirchner, I., Robock, A., Graf, H.F., Antuna, J.C., Grainger, R.G., Lambert, A., Thomason, L. Radiative forcing from the 1991 Mount Pinatubo volcanic eruption. J. Geophys. Res. Atmos. 1998;103:13837–13857.

[13] Painter, T.H., Deems, J.S., Belnap, J., Hamlet, A.F., Landry, C.C., Udall, B. Response of Colorado River runoff to dust radiative forcing in snow. Proc. Natl. Acad. Sci. U. S. A. 2010;107(40):17125–17130. DOI: 10.1073/pnas.0913139107

[14] Flanner, M.G., Zender, C.S., Randerson, J.T., Rasch, P.J. Present-day climate forcing and response from black carbon in snow. J. Geophys. Res. Atmos. 2007; pp. 1–17 112(D11). DOI: 10.1029/2006JD008003

[15] Driedger, C. Effect of ash thickness on snow ablation. In: Lipman, P.W., Christiansen, R.L., editors. The 1980 Eruptions of Mount St. Helens. Washington, DC, 1981. pp. 757–760.

[16] Dadic, R., Mullen, P.C., Schneebeli, M., Brandt, R.E., Warren, S.G. Effects of bubbles, cracks, and volcanic tephra on the spectral albedo of bare ice near the Transantarctic

Mountains: Implications for sea glaciers on Snowball Earth. J. Geophys. Res.: Earth Surface. 2013;118(3):1658–1676.

[17] Flanner, M.G., Gardner, A.S., Eckhardt, S., Stohl, A., Perket, J. Aerosol radiative forcing from the 2010 Eyjafjallajökull volcanic eruptions. J. Geophys. Res. Atmos. 2014. pp. 9481–9491, Vol. 119 DOI: 10.1002/2014JD021977

[18] Young, C.L., Sokolik, I.N., Flanner, M.G., Dufek, J. Surface radiative impacts of ash deposits from the 2009 eruption of Redoubt Volcano. J. Geophys. Res. Atmos. 2014;119(19) pp. 11387–11397 .

[19] Textor, C., Graf, H.F., Herzog, M., Oberhuber, J.M., Rose, W.I., Ernst, G.G.J. Volcanic particle aggregation in explosive eruption columns. Part I: Parameterization of the microphysics of hydrometeors and ash. J. Volcanol. Geotherm. Res. 2006;150:359–377. DOI: 10.1016/j.jvolgeores.2005.09.007

[20] Lathem, T.L., Kumar, P., Nenes, A., Dufek, J., Sokolik, I.N., Trail, M., Russell, A. Hygroscopic properties of volcanic ash. Geophys. Res. Lett. 2011;38(L11802) pp. 1–4 . DOI: 10.1029/2011GL047298

[21] Liu, X., Penner, J.E. Effect of Mt. Pinatubo H_2SO_4/H_2O aerosol on ice nucleation in the upper troposphere using a global chemistry and transport model (IMPACT). J. Geophys. Res. 2002;107(4141) pp. 1–18 . DOI: 10.1029/2001JD000455

[22] Jager, H., Deshler, T. Lidar backscatter to extinction, mass and area conversions for stratospheric aerosols based on midlatitude balloonborne size distribution measurements. Geophys. Res. Lett. 2002;29 pp. 1–4 . DOI: 10.1029/2002gl015609

[23] Stier, P., Feichter, J., Kinne, S., Kloster, S., Vignati, E., Wilson, J., Ganzeveld, L., Tegen, I., Werner, M., Balkanski, Y., Schulz, M., Boucher, O., Minikin, A., Petzold, A. The aerosol-climate model echam5-ham. Atmos. Chem. Phys. 205;5:1125–1156.

[24] Rose, W.I., Durant, A.J. Fine ash content of explosive eruptions. J. Volcanol. Geotherm. Res. 2009;186(1–2):32–39. DOI: 10.1016/j.jvolgeores.2009.01.010

[25] Prata, A.J., Bernardo, C. Retrieval of volcanic SO_2 column abundance from atmospheric infrared sounder data. J. Geophys. Res. Atmos. 2007;112 pp. 1–17 . DOI: 10.1029/2006JD007955

[26] Draxler, R.R., Rolph, G.D. NOAA Air Resources Laboratory, College Park, MD. HYSPLIT (Hybrid Single-Particle Lagrangian Integrated Trajectory) Model access via NOAA ARL READY Website [Internet]. Available at: http://www.arl.noaa.gov/HYSPLIT.php

[27] Rolph, G.D. Real-time Environmental Applications and Display System (READY) Website. NOAA Air Resources Laboratory, College Park, MD. [Internet]. Available at: http://www.ready.noaa.gov

[28] Telling, J., Flower, V.J.B., Carn, S.A. A multi-sensor satellite assessment of SO_2 emissions from the 2012–13 eruption of Plosky Tolbachik Volcano, Kamchatka. J. Volcanol. Geotherm. Res. 2015;307:98–106. DOI: 10.1016/j.volgeores.2015.07.010

[29] Young, C.L., Sokolik, I.N., Dufek, J. Regional radiative impact of volcanic aerosol from the 2009 eruption of Mt. Redoubt. Atmos. Chem. Phys. 2012;12(8):3699–3715. DOI: 10.5194/acp-12-3699-20.

[30] Wen, S., Rose, W.I. Retrieval of sizes and total masses of particles in volcanic clouds using AVHRR bands 4 and 5. J. Geophys. Res. Atmos. 1994;99(D3):5421–5431.

[31] Rose, W.I., Delene, D.J., Schneider, D.J., Bluth, G.J.S., Krueger, A.J., Sprod, I., McKee, C., Davies, H.L., Ernst, G.G.J. Ice in the 1994 Rabaul eruption cloud: Implications for volcano hazard and atmospheric effects. Nature. 1995;375(477–479).

[32] Hess, M., Koepke, P., Schult, I. Optical properties of aerosols and clouds: The software package OPAC. B. Am. Meteorol. Soc. 1998;79:831–844.

[33] Yue, G.K., Poole, L.R., Wang, P.H., Chiou, E.W. Stratospheric aerosol acidity, density, and refractive-index deduced from SAGE-II and NMC temperature data. J. Geophys. Res. Atmos. 1994;99:3727–3738.

[34] Pollack, J.B., Toon, O.B., Khare, B.N. Optical properties of terrestrial rocks and glasses. Icarus. 1973;19:372–389.

[35] Kearney, C.S., Watson, I.M. Correcting satellite-based infrared sulphur dioxide retrievals for the presence of silicate ash. J. Geophys. Res. Atmos. 2009;114(D22208) pp. 1–12 . DOI: 10.1029/2008jd011407

[36] Fu, Q., Thorsen, T.J., Su, J., Ge, J.M., Huang, J.P. Test of Mie-based single-scattering properties of non-spherical dust aerosols in radiative flux calculations. J. Quant. Spectrosc. Radiat. Transfer. 2009;110(14):1640–1653. DOI: 10.1016/j.jqsrt.2009.03.010

[37] Quinn, P.K., Shaw, G., Andrews, E., Dutton, E.G., Ruoho-Airola, T., Gong, S.L. Arctic haze: Current trends and knowledge gaps. Tellus B. 2007;59:99–114. DOI: 10.1111/j.1600-0889.2006.00238.x

[38] Ritter, C., Notholt, J., Fischer, J., Rathke, C. Direct thermal radiative forcing of tropospheric aerosol in the arctic measured by ground based infrared spectrometry. Geophys. Res. Lett. 2005;32:L23816. DOI: 10.1029/2005gl024331

[39] Myhre, C.L., Toledano, C., Myhre, G., Stebel, K., Yttri, K.E., Aaltonen, V., Johnsrud, M., Frioud, M., Cachorro, V., De Frutos, A., Lihavainen, H., Campbell, J.R., Chaikovsky, A.P., Shiobara, M., Welton, E.J., Torseth, K. Regional aerosol optical properties and radiative impact of the extreme smoke event in the European Arctic in spring 2006. Atmos. Chem. Phys. 2007;(7):5899–5915.

[40] Stuefer, M., Freitas, S.R., Grell, G., Webley, P., Peckham, S., McKeen, S.A., Egan, S.D. Inclusion of ash and SO_2 emissions from volcanic eruptions in WRF-Chem: Develop-

ment and some applications. Geosci. Model Dev. 2013;6(2):457–468. DOI: 10.5194/gmd-6-457-2013

[41] Costa, A., Macedonio, G., Folch, A. A three-dimensional Eulerian model for transport and deposition of volcanic ashes. Earth Planetary Sci. Lett. 2006;241(3–4):634–647. DOI: 10.1016/j.epsl.2005.11.019

[42] Wilson, L., Sparks, R.S.J., Huang, T.C., Watkins, N.D. Control of volcanic column heights by eruption energetic and dynamics. J. Geophys. Res. 1978;83(NB4):1829–1836.

[43] Wallace, K.L, Schaefer, J.R., Coombs, M.L. Character, mass, distribution, and origin of tephra-fall deposits from the 2009 eruption of Redoubt Volcano, Alaska—Highlighting the significance of particle aggregation. J. Volcanol. Geotherm. Res. 2013;259:145–169. DOI: 10.1016/j.jvolgeores.2012.09.015

[44] Mastin, L.G., Schwaiger, H., Schneider, D.J., Wallace, K.L., Schaefer, J., Denlinger, R.P. Injection, transport, and deposition of tephra during event 5 at Redoubt Volcano, 23 March, 2009. J. Volcanol. Geotherm. Res. 2013;259:201–213. DOI: 10.1016/j.jvolgeores.2012.04.025

[45] Schmehl, K.J., Haupt, S.E., Pavolonis, M.J. A genetic algorithm variational approach to data assimilation and application to volcanic emissions. Pure Appl. Geophys. 2012;169(3):519–537. DOI: 10.1007/s00024-011-0385-0

[46] Young, C.L., Dufek, J., Sokolik, I.N. Assessment of depositional ash loading from the 2009 eruption of Mt. Redoubt. J. Volcanol. Geotherm. 2014;274:122–138.

[47] Rose, W.I., Chesner, C.A. Dispersal of ash in the great Toba eruption, 75 ka. Geology. 1987;15(10):913–917. DOI: 10.1130/0091-7613(1987)15<913:DOAITG>2.0.CO;2

[48] Bonadonna, C., Genco, R., Gouhier, M., Pistolesi, M., Cioni, R., Alfano, F., Hoskuldsson, A., Ripepe, M. Tephra sedimentation during the 2010 Eyjafallajokull eruption (Iceland) from deposit, radar, and satellite observations. J. Geophys. Res. Sol. Ea. 2011;116 pp. 1–20. DOI: 10.1029/2011JB008462

[49] Bonadonna, C., Connor, C.B., Houghton, B.F., Connor, L., Byrne, M., Laing, A., Hincks, T.K. Probabilistic modelling of tephra dispersal: Hazard assessment of a multiphase rhyolitic eruption at Tarawera, New Zealand. J. Geophys. Res. Sol. Ea. 2005;110(B3) pp. 1–21 . DOI: 10.1029/2003/JB002896

[50] Schaefer, J.R. The 2009 eruption of Redoubt Volcano, Alaska, with contributions by Bull, K.P., Cameron, C.E., Coombs, M.L., Diefenbach, A.K., Lopez, T., McNutt, S.R., Neal, C.A., Payne, A.L., Power, J.A., Schneider, D.J., Scott, W.E., Snedigar, S.F., Thompson, G., Wallace, K.L., Waythomas, C.F., Webley, P.W., Werner, C.A. Report of Investigations RI 2011-5, State of Alaska, Department of Natural Resources, Division of Geological and Geophysical Surveys, Fairbanks, Alaska. 2011;5:45.

[51] Steensen, T., Stuefer, M., Webley, P., Grell, G., Freitas, S. Qualitative comparison of Mount Redoubt 2009 volcanic clouds using the PUFF and WRF-Chem dispersion

models and satellite remote sensing data. J. Volcanol. Geotherm. Res. 2013;259:235–247. DOI: 10.1016/j.jvolgeores.2012.02.018

[52] Telling, J.W., Dufek, J., Shaikh, A. Ash aggregation in explosive volcanic eruptions. Geophys. Res. Lett. 2013;40(10):2355–2360. DOI: 10.1002/grl.50376

[53] Dufek, J., Manga, M., Patel, A. Granular disruption during explosive volcanic eruptions. Nat. Geosci. 2012;5:561–564.

[54] Gislason, S.R., Hassenkam, T., Nedel, S., Bovet, N., Eiriksdottir, E.S., Alfredsson, H.A., Hem, C.P., Balogh, Z.I., Dideriksen, K., Oskarsson, N., Sigfusson, B., Larsen, G., Stipp, S.L.S. Characterization of Eyjafjallajokull volcanic ash particles and a protocol for rapid risk assessment. Proc. Natl. Acad. Sci. U. S. A. 2011;108:7307–7312. DOI: 10.1073/pnas.1015053108

[55] Marzano, F., Barbieri, S., Picciotti, E., Karlsdóttir, S. Monitoring subglacial volcanic eruption using ground-based C-band radar imagery. IEEE Trans. Geosci. Remote Sensing. 2010;48:403–414.

[56] Taddeucci, J., Scarlato, P., Montanaro, C., Cimarelli, C., Del Bello, E., Freda, C., Andronico, D., Gudmundsson, M.T., Dingwell, D.B. Aggregation-dominated ash settling from the Eyjafjallajkull volcanic cloud illuminated by field and laboratory high-speed imaging. Geology. 2011;39(9):891–894. DOI: 10.1130/G32016.1

[57] Gilbert, J.S., Lane, S.J. The origin of accretionary lapilli. Bull. Volcanol. 1994;56:398–411. DOI: 10.1007/BF00326465

[58] Gilbert, J.S., Lane, S.J., Sparks, R.S.J., Koyaguchi, T. Charge measurements on particle fallout from volcanic plume. Nature. 1991;349:598–600. DOI: 10.1038/349598a0

[59] Costa, A., Folch, A., Macedonio, G. A model for wet aggregation of ash particles in volcanic plumes and clouds: 1. Theoretical formulation. J. Geophys. Res. 2010;115 pp. 1–14. DOI: 10.1029/2009JB007175

[60] Warren, S.G., Brandt, R.E., Grenfell, T.C. Visible and near-ultraviolet absorption spectrum of ice from transmission of solar radiation into snow. Appl. Opt. 2006;45(21): 5320–5334.

[61] Painter, T.H., Dozier, J., Roberts, D.A., Davis, R.E., Green, R.O. Retrieval of subpixel snow-covered area and grain size from imaging spectrometer data. Remote Sensing Environ. 2003;85(1):64–77.

[62] Clarke, A.D., Noone, K.J. Soot in the Arctic snowpack: A cause for perturbations in radiative transfer. Atmos. Environ. 1985;19(12):2045–2053.

[63] Wang, L., Li, Z., Tian, Q., Ma, Y., Zhang, F., Zhang, Y., Li, D., Li, K., Li, L. Estimate of aerosol absorbing components of black carbon, brown carbon, and dust from ground-based remote sensing data of sun-sky radiometers. J. Geophys. Res. Atmos. 2013;118:6534–6543. DOI: 10.1002/jgrd.50356

[64] Skiles, S.M., Painter, T.H., Deems, J.S., Bryant, A.C., Landry, C.C. Dust radiative forcing in snow of the Upper Colorado River Basin: 2. Interannual variability in radiative forcing and snowmelt rates. Water Resources Res. 2012;48(7) pp. 1–11 .

[65] Smith, A.J.A., Grainger, R.G. Does variation in mineral composition alter the short-wave light scattering properties of desert dust aerosol? J. Quant. Spectrosc. Radiat. Transfer. 2014;133:235–243. DOI: 10.1016/j.jqsrt.2013.08.005

[66] Zdanowicz, C.M., Zielinski, G.A., Wake, C.P. Characteristics of modern atmospheric dust deposition in snow on the Penny Ice Cap, Baffin Island, Arctic Canada. Tellus B. 1998;50(5):506–520. DOI: 10.1034/j.1600-0889.1998.t01-1-00008.x

[67] Melloh, R.A. A synopsis and comparison of selected snowmelt algorithms. Hanover, NH: Cold Regions Research and Engineering Lab; 1999. No. CRREL-99-8.

[68] Qian, Y., Gustafson, W.I., Leung, L.R., Ghan, S.J. Effects of soot-induced snow albedo change on snowpack and hydrological cycle in western United States based on Weather Research and Forecasting chemistry and regional climate simulations. J. Geophys. Res. Atmos. 2009;114(D3) pp. 1–19 . DOI: 1029/2008JD011039

[69] Sokolik, I.N., Curry, J.A., Radionov, V. Interactions of Arctic aerosols with land-cover and land-use changes in northern Eurasia and their role in the Arctic climate system. In: Gutman, G., Reissell, A., editors. Arctic Land-Cover and Land-Use in a Changing Climate: Focus on Eurasia. Springer; New York, USA, 2011.

[70] Anisimov, O.A., Vaughan, D.G., Callaghan, T.V., Furgal, C., Marchant, H., Prowse, T.D., Vilhjálmsson, H., Walsh, J.E. Polar regions (Arctic and Antarctic). In: Parry, M.L., Canziani, O.F., Palutikof, J.P., Van der Linden, P.J., Hanson, C.E., editors. Climate Change 2007: Impacts, Adaptation and Vulnerability. Contribution of Working Group II to the Fourth Assessment Report of the Intergovernmental Panel on Climate Change. Cambridge University Press; Cambridge, England, 2007. pp. 653–685.

[71] Lohmann, U., Karcher, B., Timmreck, C. Impact of the Mount Pinatubo eruption on cirrus clouds formed by homogeneous freezing in the ECHAM4 GCM. J. Geophys. Res. Atmos. 2003;108(4568) pp. 1–13 . DOI: 10.1029/2002jd003185

[72] Yadav, R. Basin specificity of climate change in western Himalaya, India: Tree-ring evidences. Curr. Sci. 2007;92(10):1424–1429.

[73] Duggen, S., Croot, P., Schacht, U., Hoffmann, L. Subduction zone volcanic ash can fertilize the surface ocean and stimulate phytoplankton growth: Evidence from biogeochemical experiments and satellite data. Geophys. Res. Lett. 2007;34(L01612) pp. 1–5 . DOI: 10.1029/2006GL027522

[74] Langmann, B., Zaksek, K., Hort, M., Duggen, S. Volcanic ash as fertilizer for the surface ocean. Atmos. Chem. Phys. 2010;10:3891–3899.

[75] Durant, A.J., Villarosa, G., Rose, W.I., Delmelle, P., Prata, A.J., Viramonte, J.G. Long-range volcanic ash transport and fallout during the 2008 eruption of Chaitén Volcano, Chile. Phys. Chem. Earth. 2012;45–46:50–64. DOI: 10.1016/j.pce.2011.09.004

[76] Jones, C.D., Cox, P.M. Modeling of the volcanic signal in the atmospheric CO_2 record. Global Biogeochem. Cycles 2001;15(2):453–465. DOI: 10.1029/2000GB001281

[77] Frölicher, T.L., Joos, F., Raible, C.C., Sarmiento, J.L. Atmospheric CO_2 response to volcanic eruptions: The role of ENSO, season, and variability. Global Biogeochem. Cycles 2013;27:239–251. DOI: 10.1002/gbc.20028

[78] Oppenheimer, C. Climatic, environmental and human consequences of the largest known historic eruption: Tambora Volcano (Indonesia) 1815. Prog. Phys. Geog. 2003;27(2):230–259. DOI: 10.1191/0309133303pp379ra

[79] Gu, L., Baldocchi, D.D., Wofsy, S.C., Munger, J.W., Michalsky, J.J., Urbanski, S.P., Boden, T.A. Response of a deciduous forest to the Mount Pinatubo eruption: Enhanced photosynthesis. Science. 2003;299(5615):2035–2038.

[80] Olgun, N., Duggen, S., Andronico, D., Kutterolf, S., Croot, P.L., Giammanco, S., Censi, P., Randazzo, L. Possible impacts of volcanic ash emissions of Mount Etna on the primary productivity in the oligotrophic Mediterranean Sea: Results from nutrient-release experiments in seawater. Mar. Chem. 2013;152:32–42. DOI: 10.106/j.marchem. 2013.04.004

[81] Rothenberg, D., Mahowald, N., Lindsay, K., Doney, S.C., Moore, J.K., Thornton, P. Volcano impacts on climate and biogeochemistry in a coupled carbon-climate model. Earth Syst. Dyn. 2012;3:121–136. DOI: 10.5194/esd-3-121-2012

[82] Dufek, J., Bergantz, G.W. Suspended load and bed-load transport of particle-laden gravity currents: The role of particle-bed interaction. Theor. Comp. Fluid Dyn. 2007;21:119–145. DOI: 10.1007/s00162-007-0041-6

IntechOpen